# A SELF-CALIBRATION METHOD FOR TERRESTRIAL LASER SCANNER

Tengfei Zhou (1), Xiaojun Cheng (1), Rui Shan (1) (2)

[1] College of Survey and Geo-Informatics, Tongji University, Shanghai 200092, China
[2] Qingdao Institute of Marine Geology, China Geological Survey, Qingdao 266071, China
Email: tfzhou5713@163.com; cxj@tongji.edu.cn; shanrui416@163.com

**KEY WORDS**: Systematic error; Self-calibration method; Non-linear model; Gauss-Newton method

**ABSTRACT:** In the process of point cloud data acquisition, the Terrestrial Laser Scanner (TLS) is often affected by many factors, such as the instrument itself, the external environment, the scanning target, etc. These factors reduce the observation accuracy of point cloud coordinates to a certain extent, making the obtained coordinates and the real coordinates of the measured points not corresponded, which directly influences the results of subsequent point cloud processing. In this paper, a new self-calibration model of scanner is established based on the observation principle of TLS technology and the similarity transformation model to analyse the range error and angle error of the scanner, so as to weaken the influence of system error on point cloud coordinate sequences. In addition, the new scheme can take into account the random errors in the observation vectors. Finally, based on the non-linear Gauss-Helmert model and the total least squares theory, the Gauss-Newton iteration algorithm is used to solve the system error parameters and conversion parameters. The experimental results show that, compared with the traditional coordinates transformation scheme, the coordinate sequence accuracy after system error correction is higher and closer to the real value.

## 1. INTRODUCTION

TLS technology adopts non-contact measurement method, which can quickly acquire massive point cloud data on the target surface in a short time. In recent years, it has been widely used in three-dimensional reconstruction, cultural relics protection, deformation monitoring, digital city and other fields. Compared with the traditional single-point acquisition method, it greatly improves the work efficiency and measurement accuracy.

Three-dimensional data of laser point cloud is calculated based on polar coordinate system according to the oblique distance, horizontal and vertical angles obtained by the instrument. In the measurement process of TLS, systematic errors such as ranging, angle measurement, incident angle, target reflectivity and temperature are indispensable. These errors directly determine the accuracy of point cloud data, and to some extent, weaken the accuracy of subsequent point cloud processing. Usually, users can correct or evaluate the results of scanning measurement according to the application environment and nominal accuracy of the instrument, but the actual scanning accuracy of the instrument does not always correspond to the nominal accuracy, so it is necessary to make a reasonable determination.

Based on the observation equation of the scanner, (Zhang Yi et al., 2012) established a system error model, and realized the overall solution of the system error and conversion parameters by using spatial similarity transformation. (Mao Aiquan et al., 2014) studied the ranging error rule of the TLS by using high-precision baseline calibration field, and deduced the error correction modes of the additive constant and multiplicative constant. The additive constant and multiplication constant of laser scanner are obtained by baseline comparison method by (Liu Chun et al., 2009), and the angle measurement accuracy is tested by using the method of shafting error correction of total station. After calibration, the instrument can reach the nominal accuracy. (Xie Hongquan et al., 2014) used the angle measurement data of total station as the reference to study the horizontal angle observation accuracy of scanner under different distance conditions. Based on the principle of scanner ranging and error sources, (Zhao Song et al., 2013) established a ranging error model via the intensity of return light; (Xie Rui et al., 2008) analyzed and studied the point position accuracy of scanner under different experimental conditions, pointed out that the scanning distance error increases with distance. Angle, reflector and environmental factors are not the fundamental sources of midpoint error. Furthermore, The midpoint error is mainly caused by the instrument itself. (Guan Yunlan et al., 2014) constructed a self-calibration model of ground laser scanner with 11 parameters on the basis of spatial similarity transformation, and carried out systematic error calibration for HDS3000 scanner. For AM-CW TLS system, (Derek D, 2006) proposed a rigorous method for TLS self-calibration using a network of signalized points by adding a set of additional parameters; (Xiaolu Li et al., 2018) established an angle measurement error model by the ray-tracing method involves five types of mounting angle errors, to calibrate a lab-built terrestrial laser scanner; (J. C. K. Chow et al.,2012) used different primitives to calibrate Leica HDS6100 and Trimble GS200 scanner.

Based on the observation equation of TLS and the theory of spatial similarity transformation, a self-calibration model of scanner with 12 parameters is constructed, including three translation parameters, three rotation parameters, one scale parameter and five instrument system error parameters. Finally, the Gauss-Newton iteration method from (Shen Y et al., 2011) is used to solve the conversion parameters and system errors, simultaneously.

## 2. SELF-CALIBRATION MODEL

The ground laser scanner uses an independent right-handed coordinate system. Its original point is located in the center of the scanner. The X-axis is in the transverse scanning plane. The Y-axis is perpendicular to the X-axis in the transverse scanning plane, and the Z-axis is perpendicular to the X-Y plane. The original observation data of TLS are slant distance $s$, horizontal angle $\theta$ and vertical angle $\alpha$, i.e. $(s, \theta, \alpha)$, which belong to polar coordinate system.

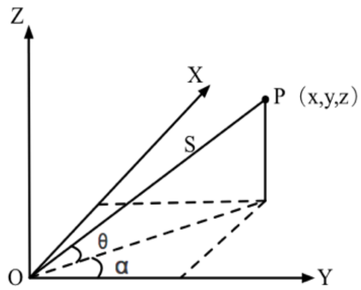


Figure 1 Polar coordinate system

In order to obtain the three-dimensional coordinates of the target point relative to the origin, it is necessary to transform the original observation value into Cartesian coordinate system. Equation (1) is the transformation model for the above two coordinate system, i.e. the observation equation of TLS.

$$\left.\begin{aligned} x &= s\cdot\cos\theta\cdot\cos\alpha \\ y &= s\cdot\cos\theta\cdot\sin\alpha \\ z &= s\cdot\sin\theta \end{aligned}\right\} \tag{1}$$

For scanning at different stations, according to the observation equation of TLS, although the factors of target and environment are different, the influence on scanning results is shown in the systematic errors of ranging and angle measurement (Zhang Yi et al., 2012). Similar to the total station, because the scanner uses photoelectric ranging method, there are two kinds of systematic errors in ranging: adding constant $m$ and multiplying constant $\lambda$. Owing to the errors in the manufacture and installation of the instrument and the changes in the course of its use, there are usually collimation axis error $c$ and horizontal axis error $i$ in horizontal angle observation. Besides, there is vertical index error $\delta$ in vertical angle observation.

The correction results of collimation axis error $c$ and horizontal axis error $i$ to horizontal angle observations can be expressed as below:

$$\left.\begin{aligned} c' &= c/\cos\theta \\ i' &= i\cdot\tan\theta \end{aligned}\right\} \tag{2}$$

The self-calibration scheme proposed in this paper is based on the similarity transformation model. These system errors in the point cloud data are all taken as unknowns, then it is solved by indirect adjustment theory with conversion parameters as a whole. The self-calibration model consists of 12 parameters, namely, 5 system error parameters, 3 translation parameters, 3 rotation parameters and 1 scale parameter. The function model of self-calibration method is as follows:

$$\begin{bmatrix} X \\ Y \\ Z \end{bmatrix} - \begin{bmatrix} e_X \\ e_Y \\ e_Z \end{bmatrix} = \mu\boldsymbol{R}\begin{bmatrix} x-e_x \\ y-e_y \\ z-e_z \end{bmatrix} + \begin{bmatrix} \Delta x \\ \Delta y \\ \Delta z \end{bmatrix} \tag{3}$$

where $[X \quad Y \quad Z]^{\mathrm{T}}$ and $[x \quad y \quad z]^{\mathrm{T}}$are the coordinate observation vectors of the scanning points in the adjacent stations. $[e_X \quad e_Y \quad e_Z]^{\mathrm{T}}$ and $[e_x \quad e_y \quad e_z]^{\mathrm{T}}$ represent the random errors of the corresponding observation vectors. $\mu$ is the scaling transformation parameters. $[\Delta x \quad \Delta y \quad \Delta z]^{\mathrm{T}}$ is the translation parameters, and $\boldsymbol{R}$ is the rotation matrix, computed as below:

$$\boldsymbol{R} = \boldsymbol{R}_1\cdot\boldsymbol{R}_2\cdot\boldsymbol{R}_3 \tag{4}$$

$$\boldsymbol{R}_1=\begin{bmatrix}\cos\varphi & 0 & -\sin\varphi\\ 0 & 1 & 0\\ \sin\varphi & 0 & \cos\varphi\end{bmatrix},\boldsymbol{R}_2=\begin{bmatrix}1 & 0 & 0\\ 0 & \cos\omega & -\sin\omega\\ 0 & \sin\omega & \cos\omega\end{bmatrix},\boldsymbol{R}_3=\begin{bmatrix}\cos\kappa & -\sin\kappa & 0\\ \sin\kappa & \cos\kappa & 0\\ 0 & 0 & 1\end{bmatrix} \tag{5}$$

where $(\varphi, \omega, \kappa)$ is the rotation parameter vector, i.e. the Euler angles rotating around the Y axis, the X axis and the Z axis, respectively. The least square algorithm can effectively eliminate the influence of random errors in point cloud data but not systematic errors. Considering the Eqs. (1) - (3), the self-calibration function model can be abstracted as a kind of EIV model:

$$\boldsymbol{X}_2-\boldsymbol{e}_2=\mu\boldsymbol{R}\left(\boldsymbol{X}_1-\boldsymbol{e}_1\right)+\Delta\boldsymbol{X} \tag{6}$$

where

$$\left.\begin{aligned}&\boldsymbol{X}_2=\begin{bmatrix}X & Y & Z\end{bmatrix}^{\mathrm{T}},\boldsymbol{e}_2=\begin{bmatrix}e_X & e_Y & e_Z\end{bmatrix}^{\mathrm{T}}\\ &\boldsymbol{e}_1=\begin{bmatrix}e_x & e_y & e_z\end{bmatrix}^{\mathrm{T}},\Delta\boldsymbol{X}=\begin{bmatrix}\Delta x & \Delta y & \Delta z\end{bmatrix}^{\mathrm{T}}\\ &\boldsymbol{X}_1=\begin{bmatrix}x\\ y\\ z\end{bmatrix}=\begin{bmatrix}\left(s+m+\lambda s\right)\cos\left(\theta+\delta\right)\cos\left(\alpha+c'+i'\right)\\ \left(s+m+\lambda s\right)\cos\left(\theta+\delta\right)\sin\left(\alpha+c'+i'\right)\\ \left(s+m+\lambda s\right)\sin\left(\theta+\delta\right)\end{bmatrix}\end{aligned}\right\} \tag{7}$$

The parameter vector is:

$$\boldsymbol{x}=\begin{bmatrix}\Delta x & \Delta y & \Delta z & \mu & \varphi & \omega & \kappa & m & \lambda & c & i & \delta\end{bmatrix}^{\mathrm{T}} \tag{8}$$

## 3. DERIVATION OF SELF-CALIBRATION MODEL

Since the self-calibration model is a non-linear model essentially, the Gauss-Newton method of non-linear least squares is adopted to derive the solution. We assume that the approximate values of $\boldsymbol{e}_1$ and $\boldsymbol{e}_2$ are $\boldsymbol{e}_1^0$ and $\boldsymbol{e}_2^0$, respectively. The parameters' approximate values of the self-calibration model are set up as:

$$\boldsymbol{x}^0=\begin{bmatrix}\Delta x^0 & \Delta y^0 & \Delta z^0 & \mu^0 & \varphi^0 & \omega^0 & \kappa^0 & m^0 & \lambda^0 & c^0 & i^0 & \delta^0\end{bmatrix}^{\mathrm{T}} \tag{9}$$

The right-hand members of Eq. (6) is expanded at $(x^0, \boldsymbol{e}_1^0, \boldsymbol{e}_2^0)$ through Taylor series as:

$$\begin{aligned}\boldsymbol{F}=\boldsymbol{X}_2-\boldsymbol{e}_2&=\mu^0\boldsymbol{R}^0\left(\boldsymbol{X}_1^0-\boldsymbol{e}_1\right)+\Delta\boldsymbol{X}^0+\mu^0\left(\frac{\partial\boldsymbol{R}}{\partial\varphi}d\varphi+\frac{\partial\boldsymbol{R}}{\partial\omega}d\omega+\frac{\partial\boldsymbol{R}}{\partial\kappa}d\kappa\right)\left(\boldsymbol{X}_1^0-\boldsymbol{e}_1^0\right)\\ &+\begin{bmatrix}d\Delta x\\ d\Delta y\\ d\Delta z\end{bmatrix}+\boldsymbol{R}^0\left(\boldsymbol{X}_1^0-\boldsymbol{e}_1^0\right)d\mu+\frac{\partial\boldsymbol{F}}{\partial m}dm+\frac{\partial\boldsymbol{F}}{\partial\lambda}d\lambda+\frac{\partial\boldsymbol{F}}{\partial c}dc+\frac{\partial\boldsymbol{F}}{\partial i}di+\frac{\partial\boldsymbol{F}}{\partial\delta}d\delta\end{aligned} \tag{10}$$

where

$$\left.\begin{aligned}\frac{\partial\boldsymbol{R}}{\partial\varphi}&=\frac{\partial\boldsymbol{R}_1}{\partial\varphi}\boldsymbol{R}_2\boldsymbol{R}_3=\begin{bmatrix}-\sin\varphi & 0 & -\cos\varphi\\ 0 & 0 & 0\\ \cos\varphi & 0 & -\sin\varphi\end{bmatrix}\begin{bmatrix}1 & 0 & 0\\ 0 & \cos\omega & -\sin\omega\\ 0 & \sin\omega & \cos\omega\end{bmatrix}\begin{bmatrix}\cos\kappa & -\sin\kappa & 0\\ \sin\kappa & \cos\kappa & 0\\ 0 & 0 & 1\end{bmatrix}\\ \frac{\partial\boldsymbol{R}}{\partial\omega}&=\boldsymbol{R}_1\frac{\partial\boldsymbol{R}_2}{\partial\omega}\boldsymbol{R}_3=\begin{bmatrix}\cos\varphi & 0 & -\sin\varphi\\ 0 & 1 & 0\\ \sin\varphi & 0 & \cos\varphi\end{bmatrix}\begin{bmatrix}0 & 0 & 0\\ 0 & -\sin\omega & -\cos\omega\\ 0 & \cos\omega & -\sin\omega\end{bmatrix}\begin{bmatrix}\cos\kappa & -\sin\kappa & 0\\ \sin\kappa & \cos\kappa & 0\\ 0 & 0 & 1\end{bmatrix}\end{aligned}\right\}$$

$$
\left.\begin{aligned}
&\frac{\partial \boldsymbol{R}}{\partial \kappa}=\boldsymbol{R}_1\boldsymbol{R}_2\frac{\partial \boldsymbol{R}_3}{\partial \kappa}=\begin{bmatrix}\cos\varphi & 0 & -\sin\varphi\\ 0 & 1 & 0\\ \sin\varphi & 0 & \cos\varphi\end{bmatrix}\begin{bmatrix}1 & 0 & 0\\ 0 & \cos\omega & -\sin\omega\\ 0 & \sin\omega & \cos\omega\end{bmatrix}\begin{bmatrix}-\sin\kappa & -\cos\kappa & 0\\ \cos\kappa & -\sin\kappa & 0\\ 0 & 0 & 0\end{bmatrix}\\
&\frac{\partial \boldsymbol{F}}{\partial m}=\mu^0\boldsymbol{R}^0\begin{bmatrix}\cos\left(\theta+\delta^0\right)\cos\left(\alpha+c'^0+i'^0\right)\\ \cos\left(\theta+\delta^0\right)\sin\left(\alpha+c'^0+i'^0\right)\\ \sin\left(\theta+\delta^0\right)\end{bmatrix}\\
&\frac{\partial \boldsymbol{F}}{\partial \lambda}=\mu^0\boldsymbol{R}^0\begin{bmatrix}s\cdot\cos\left(\theta+\delta^0\right)\cos\left(\alpha+c'^0+i'^0\right)\\ s\cdot\cos\left(\theta+\delta^0\right)\sin\left(\alpha+c'^0+i'^0\right)\\ s\cdot\sin\left(\theta+\delta^0\right)\end{bmatrix}\\
&\frac{\partial \boldsymbol{F}}{\partial c}=\mu^0\boldsymbol{R}^0\begin{bmatrix}-\left(s+m^0+\lambda^0 s\right)\cos\left(\theta+\delta^0\right)\sin\left(\alpha+c'^0+i'^0\right)\\ \left(s+m^0+\lambda^0 s\right)\cos\left(\theta+\delta^0\right)\cos\left(\alpha+c'^0+i'^0\right)\\ 0\end{bmatrix}\cdot\frac{1}{\cos\theta}\\
&\frac{\partial \boldsymbol{F}}{\partial i}=\mu^0\boldsymbol{R}^0\begin{bmatrix}-\left(s+m^0+\lambda^0 s\right)\cos\left(\theta+\delta^0\right)\sin\left(\alpha+c'^0+i'^0\right)\\ \left(s+m^0+\lambda^0 s\right)\cos\left(\theta+\delta^0\right)\cos\left(\alpha+c'^0+i'^0\right)\\ 0\end{bmatrix}\cdot\tan\theta\\
&\frac{\partial \mathbf{F}}{\partial \delta}=\mu^0\mathbf{R}^0\begin{bmatrix}-\left(s+m^0+\lambda^0 s\right)\sin\left(\theta+\delta^0\right)\cos\left(\alpha+c'^0+i'^0\right)\\ -\left(s+m^0+\lambda^0 s\right)\sin\left(\theta+\delta^0\right)\sin\left(\alpha+c'^0+i'^0\right)\\ \left(s+m^0+\lambda^0 s\right)\cos\left(\theta+\delta^0\right)\end{bmatrix}
\end{aligned}\right\} \tag{11}
$$

By substituting Eq. (11) into Eq. (10) and Eq. (10) can be sort out as following:

$$
\boldsymbol{X}_2-\boldsymbol{e}_2=\mu^0\boldsymbol{R}^0\boldsymbol{X}_1^0+\Delta\boldsymbol{X}^0+\boldsymbol{A}^0 d\boldsymbol{x}-\mu^0\boldsymbol{R}^0\boldsymbol{e}_1 \tag{12}
$$

where $d\boldsymbol{x}$ and $\boldsymbol{A}^0$ represent the correction vector matrix of the parameters and coefficient matrix, respectively. Considering Eqs. (9) - (11), $d\boldsymbol{x}$ and $\boldsymbol{A}^0$ can be expressed as:

$$
\left.\begin{aligned}
&d\boldsymbol{x}=\begin{bmatrix} d\Delta x & d\Delta y & d\Delta z & d\mu & d\varphi & d\omega & d\kappa & dm & d\lambda & dc & di & d\delta\end{bmatrix}^{\mathrm{T}}\\
&\boldsymbol{A}^0=\begin{bmatrix}\boldsymbol{E}_{3\times3} & \begin{pmatrix}\boldsymbol{R}^0 & \mu^0\dfrac{\partial \boldsymbol{R}}{\partial \varphi} & \mu^0\dfrac{\partial \boldsymbol{R}}{\partial \omega} & \mu^0\dfrac{\partial \boldsymbol{R}}{\partial \kappa}\end{pmatrix}\left(\boldsymbol{X}_1^0-\boldsymbol{e}_1^0\right) & \dfrac{\partial \boldsymbol{F}}{\partial m} & \dfrac{\partial \boldsymbol{F}}{\partial \lambda} & \dfrac{\partial \boldsymbol{F}}{\partial c} & \dfrac{\partial \boldsymbol{F}}{\partial i} & \dfrac{\partial \boldsymbol{F}}{\partial \delta}\end{bmatrix}
\end{aligned}\right\} \tag{13}
$$

The Lagrange objective function of self-calibration model is constructed as below:

$$
\Phi\left(\boldsymbol{e}_1,\boldsymbol{e}_2,d\boldsymbol{x},\boldsymbol{K}\right)=\boldsymbol{e}_1^{\mathrm{T}}\boldsymbol{Q}_1^{-1}\boldsymbol{e}_1+\boldsymbol{e}_2^{\mathrm{T}}\boldsymbol{Q}_2^{-1}\boldsymbol{e}_2+2\boldsymbol{K}^{\mathrm{T}}\left(\boldsymbol{X}_2-\boldsymbol{e}_2-\mu^0\boldsymbol{R}^0\boldsymbol{X}_1^0-\Delta\boldsymbol{X}^0-\boldsymbol{A}^0 d\boldsymbol{x}+\mu^0\boldsymbol{R}^0\boldsymbol{e}_1\right) \tag{14}
$$

where $\boldsymbol{K}$ is the "Lagrange multiples" with dimensions $n\times 1$. The solution of this target function can be derived by means of Euler-Lagrange necessary conditions, namely, the partial derivatives are zero after obtaining partial derivatives of each variable.

$$
\left.\frac{1}{2}\frac{\partial \Phi}{\partial \boldsymbol{e}_1}=\boldsymbol{Q}_1^{-1}\boldsymbol{e}_1+\left(\boldsymbol{R}^0\right)^{\mathrm{T}}\mu^0\boldsymbol{K}=0\right\}
$$

$$\left.\begin{aligned}&\frac{1}{2}\frac{\partial\Phi}{\partial \boldsymbol{e}_2}=\boldsymbol{Q}_2^{-1}\boldsymbol{e}_2-\boldsymbol{K}=0\\&\frac{1}{2}\frac{\partial\Phi}{\partial d\boldsymbol{x}}=-\left(\boldsymbol{A}^0\right)^{\mathrm{T}}\boldsymbol{K}=0\\&\frac{1}{2}\frac{\partial\Phi}{\partial \boldsymbol{K}}=\boldsymbol{X}_2-\boldsymbol{e}_2-\mu^0\boldsymbol{R}^0\boldsymbol{X}_1^0-\Delta\boldsymbol{X}^0-\boldsymbol{A}^0d\boldsymbol{x}+\mu^0\boldsymbol{R}^0\boldsymbol{e}_1=0\end{aligned}\right\}\tag{15}$$

According to Eq. (14) and (15), we can readily obtain the correction vector of unknown parameter as below:

$$d\boldsymbol{x}=\left(\left(\boldsymbol{A}^0\right)^{\mathrm{T}}\left(\boldsymbol{Q}_c^0\right)^{-1}\boldsymbol{A}^0\right)^{-1}\left(\boldsymbol{A}^0\right)^{\mathrm{T}}\boldsymbol{Q}_c^{-1}\boldsymbol{L}\tag{16}$$

where

$$\left.\begin{aligned}&\boldsymbol{Q}_c^0=\boldsymbol{Q}_2+\mu^0\boldsymbol{R}^0\boldsymbol{Q}_1\left(\boldsymbol{R}^0\right)^{\mathrm{T}}\mu^0\\&\boldsymbol{L}=\boldsymbol{X}_2-\mu^0\boldsymbol{R}^0\boldsymbol{X}_1^0-\Delta\boldsymbol{X}^0\end{aligned}\right\}\tag{17}$$

Thereby, the parameter vectors and random errors of observation vectors after the first ($j$+1) iteration are updated as:

$$\left.\begin{aligned}&\boldsymbol{x}^{j+1}=\boldsymbol{x}^j+d\boldsymbol{x}^{j+1}\\&\boldsymbol{e}_1^{j+1}=-\boldsymbol{Q}_1\left(\boldsymbol{R}^0\right)^T\mu^0\left(\boldsymbol{Q}_c^0\right)^{-1}\left(\boldsymbol{L}-\boldsymbol{A}^0d\boldsymbol{x}^{j+1}\right)\\&\boldsymbol{e}_2^{j+1}=\boldsymbol{Q}_2\left(\boldsymbol{Q}_c^0\right)^{-1}\left(\boldsymbol{L}-\boldsymbol{A}^0d\boldsymbol{x}^{j+1}\right)\end{aligned}\right\}\tag{18}$$

Regardless of the minimum term $\boldsymbol{A}^0d\boldsymbol{x}^{j+1}$, at the end of iteration, the sum of weighted squares of residual can be expressed as:

$$\begin{aligned}\boldsymbol{e}_1^{\mathrm{T}}\boldsymbol{Q}_1^{-1}\boldsymbol{e}_1+\boldsymbol{e}_2^{\mathrm{T}}\boldsymbol{Q}_2^{-1}\boldsymbol{e}_2&=\boldsymbol{L}^{\mathrm{T}}\left(\boldsymbol{Q}_c^0\right)^{-1}\mu^0\boldsymbol{R}^0\boldsymbol{Q}_1\boldsymbol{Q}_1^{-1}\boldsymbol{Q}_1\left(\boldsymbol{R}^0\right)^{\mathrm{T}}\mu^0\left(\boldsymbol{Q}_c^0\right)^{-1}\boldsymbol{L}+\boldsymbol{L}^{\mathrm{T}}\left(\boldsymbol{Q}_c^0\right)^{-1}\boldsymbol{Q}_2\boldsymbol{Q}_2^{-1}\boldsymbol{Q}_2\left(\boldsymbol{Q}_c^0\right)^{-1}\boldsymbol{L}\\&=\boldsymbol{L}^{\mathrm{T}}\left(\boldsymbol{Q}_c^0\right)^{-1}\left(\mu^0\boldsymbol{R}^0\boldsymbol{Q}_1\left(\boldsymbol{R}^0\right)^{\mathrm{T}}\mu^0+\boldsymbol{Q}_2\right)\left(\boldsymbol{Q}_c^0\right)^{-1}\boldsymbol{L}\\&=\boldsymbol{L}^{\mathrm{T}}\left(\boldsymbol{Q}_c^0\right)^{-1}\boldsymbol{L}\end{aligned}\tag{19}$$

As a consequence, the unit weight median error and covariance matrix of the estimated parameters can be estimated via Eqs. (19) and (16) as following:

$$\left.\begin{aligned}&\hat{\sigma}_0=\sqrt{\frac{\boldsymbol{e}_1^{\mathrm{T}}\boldsymbol{Q}_1^{-1}\boldsymbol{e}_1+\boldsymbol{e}_2^{\mathrm{T}}\boldsymbol{Q}_2^{-1}\boldsymbol{e}_2}{3n-12}}=\sqrt{\frac{\boldsymbol{L}^{\mathrm{T}}\left(\boldsymbol{Q}_c^0\right)^{-1}\boldsymbol{L}}{3n-12}}\\&\boldsymbol{D}_x=\hat{\sigma}_0^2\left(\left(\boldsymbol{A}^0\right)^{\mathrm{T}}\left(\boldsymbol{Q}_c^0\right)^{-1}\boldsymbol{A}^0\right)^{-1}\end{aligned}\right\}\tag{20}$$

The systematic error self-calibration model of TLS can be realized via the following steps:
(1) Determining the iterative initial value of the unknown parameters.
We can use the linear transformation model to obtain the initial values of transformation parameters. Or take a simpler approach that the scale parameter is set to **One**, and the translation parameter and rotation parameter are set to **Zero**. In terms of system errors, it can be considered that all kinds of errors are completely eliminated in the manufacture and installation of the instrument, and the initial value of system error can be set to **Zero** (guan et al., 2014).
(2) Iteration process
(a) Calculating the required coefficient matrix $\boldsymbol{A}$, covariance matrix $\boldsymbol{Q}_c$ and observation vector matrix $\boldsymbol{L}$ for the $i$th iteration by Eqs. (13) and (17).
(b) Predicting $d\boldsymbol{x}$, $\boldsymbol{x}$ and $\boldsymbol{e}$ through Eqs. (16) and (18).

(c) Substituting the updated $\boldsymbol{dx}$, $\boldsymbol{x}$ and $\boldsymbol{e}$ into Eqs. (13) and (17) to obtain $\boldsymbol{A}$, $\boldsymbol{Q}_c$ and $\boldsymbol{L}$ for the next iteration.
(d) Repeating (a) – (c) process until $\boldsymbol{dx}$ is less than a set positive threshold and terminate iteration.
(e) Transforming the coordinates of other points into target coordinate system based on the predicted 12 parameters.
(3) Accuracy evaluation.

## 4. EXPERIMENTS AND RESULTS

Using the measured point cloud coordinate sequence from (Guan Yunlan et al., 2014) as the experimental data. HDS3000 scanner was the experimental object, and five Faro target spheres and three target planes were scanned. The coordinates of the spherical centers and planar centers were obtained by fitting the observed values, and the target coordinate system was established by SOKKIA 1200 total station.
The scanning coordinates of the five spherical centers with the measured coordinates through the total station are taken as the same-name points to solve the parameters, then the coordinates of the three centers are corrected and transformed by using the parameters. Through the difference between the converted coordinates and the original coordinates, the mean error of coordinate components and the mean error of point positions are calculated based on the Bessel formula.

$$\hat{\sigma} = \sqrt{\boldsymbol{V}^{\mathrm{T}}\boldsymbol{V} / (n-1)} \tag{21}$$

Table 1 Coordinates Sequence of TLS and Total Station (unit: m)

| Classes | TLS | | | Total station | | |
|---|---|---|---|---|---|---|
| | x | y | z | X | Y | Z |
| Sphere1 | 3.8057 | -3.6132 | -0.4957 | 6.5368 | 10.0224 | 5.7071 |
| Sphere2 | 1.1437 | -6.5275 | -0.6502 | 2.7830 | 11.2521 | 5.5628 |
| Sphere3 | -0.6325 | -3.3331 | -0.6429 | 2.8041 | 7.5964 | 5.5640 |
| Sphere4 | -3.0580 | -3.7878 | -1.0332 | 0.4659 | 6.7989 | 5.1775 |
| Sphere5 | -3.4119 | -1.7673 | -0.6451 | 1.1509 | 4.8632 | 5.5611 |
| Plane1 | 1.6613 | -3.5856 | -0.5756 | 4.6813 | 8.9467 | 5.6292 |
| Plane2 | 0.7593 | -1.5648 | -0.5447 | 4.8888 | 6.7429 | 5.6555 |
| Plane3 | -1.7224 | -0.9954 | -0.5689 | 3.0013 | 5.0232 | 5.6314 |

The following two experimental schemes are employed to implement the prediction of transformation parameters and systematic errors.
Scheme 1, a non-linear least squares transformation algorithm without considering the systematic errors.
Scheme 2, the new scheme proposed in this paper

Table 2 Parameter Estimation Results

| Parameters | Scheme 1 | Scheme 2 |
|---|---|---|
| $\Delta X$ /m | 4.9946 | 4.9975 |
| $\Delta Y$ /m | 5.0021 | 4.9990 |
| $\Delta Z$ /m | 6.1979 | 6.1991 |
| $\mu$ | ∅ | 1.0039 |
| $\varphi$ /rad | -0.0022 | -0.0022 |
| $\omega$ /rad | 0.0016 | 0.0016 |
| $\kappa$ /rad | -1.0572 | -1.0656 |
| $m$ /m | ∅ | 0.0060 |
| $\lambda$ | ∅ | -0.0040 |
| $c$ /rad | ∅ | -0.0086 |
| $i$ /rad | ∅ | -0.0018 |
| $\delta$ /rad | ∅ | -9.1165E-05 |

where ∅ stands for null value.

Table 3 Corrected plane target coordinates (unit: m)

| Plane | Scheme 1 | | | Scheme 2 | | |
|---|---|---|---|---|---|---|
| | X | Y | Z | X | Y | Z |
| 1 | 4.6786 | 8.9422 | 5.6294 | 4.6807 | 8.9443 | 5.6294 |
| 2 | 4.8859 | 6.7389 | 5.6562 | 4.8883 | 6.7412 | 5.6556 |
| 3 | 3.0041 | 5.0238 | 5.6335 | 3.0016 | 5.0205 | 5.6330 |

According to the calculated parameters, converting planar coordinates acquired by scanner into total station coordinate system. Then, the median error of each coordinate component and the point median errors are calculated through the difference, i.e. $(dX,\ dY,\ dZ)$, between the converted coordinates and the measured coordinates.

Table 4 Coordinate differences (unit: m)

| Plane | Scheme 1 | | | Scheme 2 | | |
|---|---|---|---|---|---|---|
| | $dX$ | $dY$ | $dZ$ | $dX$ | $dY$ | $dZ$ |
| 1 | -0.0027 | -0.0045 | 0.0002 | -0.0006 | -0.0024 | 0.0002 |
| 2 | -0.0029 | -0.0040 | 0.0007 | -0.0005 | -0.0017 | 0.0001 |
| 3 | 0.0028 | -0.0006 | 0.0021 | 0.0003 | -0.0027 | 0.0016 |
| $\hat{\sigma}$ | 0.0028 | 0.0035 | 0.0013 | 0.0005 | 0.0022 | 0.0009 |
| $\hat{\sigma}_p$ | $\sigma_p = \sqrt{\left(\sigma_x^2 + \sigma_y^2 + \sigma_z^2\right)} = 0.0046$ | | | $\sigma_p = \sqrt{\left(\sigma_x^2 + \sigma_y^2 + \sigma_z^2\right)} = 0.0025$ | | |

Table 2 shows that the coordinate sequence corrected by system errors is closer to the measured coordinate data, and the error of coordinate components and points increases by 82.1%, 37.1%, 30.8% and 45.7%, respectively.

## 5. CONCLUSION

Based on the similarity transformation model and the working principle of scanner, a self-calibration model of scanner system error with 12 parameters is constructed in this paper. The corresponding iterative algorithm is deduced in detail by Gauss-Newton method. The validity of the algorithm is verified by the measured data. The results show that the point cloud sequences with system error correction is effective and point cloud data can obtain more accurate transformation coordinates. The new algorithm takes into account the random errors in the observation data at the same time, so it is more rigorous in theory than the existing algorithm. The new algorithm builds a model based on the observation principle of scanner. It has reference value in the following point cloud data processing, such as point cloud registration, coordinate transformation in geodesy, image matching and so on. In addition, there is a certain correlation between the parameters solved by the self-calibration model, so further research is needed to weaken or eliminate the correlation between the parameters.


## ACKNOWLEDGMENT

This research was supported by the Guangzhou Science and Technology Project (No. 201704030102), the National Natural Science Foundation of China (No. 41671449).


## REFERENCE


Derek D, 2010. Terrestrial laser scanner self-calibration: correlation sources and their mitigation. ISPRS Journal of Photogrammetry and Remote Sensing, 65(1), pp. 93-102.

Guan Yunlan, Cheng Xiaojun, et al., 2014. Yunlan G , Xiaojun C , Xinwu Z , et al. Research on Systematic Errors Calibration of Terrestrial Laser Scanner[J]. Acta Geodaetica et Cartographica Sinica, 43(7), pp. 731-738.

International Archives of the Photogrammetry, Remote Sensing and Spatial Information Sciences.

J. C. K. Chow, et a l., 2012. Point-based versus plane-based self-calibration of static terrestrial laser scanners. ISPRS

Liu Chun, Zhang Yunling, et al., 2009. Accuracy evaluation of 3D laser range scanner based on field calibration. Geotechnical Investigation & Surveying, (11), pp. 56-60.

Mao Aiquan, Zhu Yihu, et al., 2014. The Research of Accuracy Evaluation Method and Error Correction Model Based on 3D Laser Scanner. Bulletin of Surveying and Mappin, (2), pp. 72-75.

Shen Y., Li B., Yi C., 2011. An iterative solution of weighted total least-squares adjustment. Journal of Geodesy, 85(4), pp. 229-238.

Xiaolu Li, Yunye Li, et al., 2018. Lab-built terrestrial laser scanner self-calibration using mounting angle error correction. Optics Express, 26(11), 14444.

Xie Hongquan, Gao Xiangwei, et al., 2014. Research on Horizontal Angle Measurement Accuracy of Terrestrial 3D Laser Scanner Based on Field Calibration Test. Bulletin of Surveying and Mappin, (8), pp. 52-54.

Xie Rui, Hu Minjie, et al., 2008. Point accuracy analysis and research of three-dimensional laser HDS3000 scanner. Remote sensing information, (6), pp. 53-57.

Zhang Yi, Yan Li, et al., 2012. Research on Systematic Error Model of Terrestrial Laser Scanning. Bulletin of Surveying and Mappin, 27(1), pp. 16-19.

Zhao Song, Xi Qin, et al., 2013. Ranging Error Model of Ground 3D Laser Scanner Based on Reflective Intensity. Science of Surveying and Mapping, 38(3), pp. 169-174.